Optimal vaccination and bednet maintenance for the control of malaria in a region with naturally acquired immunity

Olivia Prosper[1]*, Nick Ruktanonchai[2]
Maia Martcheva[3]

[1]Department of Mathematics, Dartmouth College, Hanover, NH, USA,
[2]Department of Biology, University of Florida, Gainesville, FL, USA,
[3]Department of Mathematics, University of Florida, Gainesville, FL, USA

January 22, 2014

Abstract

Following over two decades of research, the malaria vaccine candidate RTS,S has reached the final stages of vaccine trials, demonstrating an efficacy of roughly 50% in young children. Regions with high malaria prevalence tend to have high levels of naturally acquired immunity (NAI) to severe malaria; NAI is caused by repeated exposure to infectious bites and results in large asymptomatic populations. To address concerns about how these vaccines will perform in regions with existing NAI, we developed a simple malaria model incorporating vaccination and NAI. Typically, if the basic reproduction number (R_0) for malaria is greater than unity, the disease will persist; otherwise, the disease will become extinct. However, analysis of this model revealed that NAI, compounded by a subpopulation with only partial protection to malaria, may render vaccination efforts ineffective and potentially detrimental to malaria control, by increasing R_0 and increasing the likelihood of malaria persistence even when $R_0 < 1$. The likelihood of this scenario increases when non-immune infected individuals are treated disproportionately compared with partially immune individuals – a plausible scenario since partially immune individuals are more likely to be asymptomatically infected. Consequently, we argue that active case-detection of asymptomatic infections is a critical component of an effective malaria control program. We then investigated optimal vaccination and bed net control programs under two endemic settings with varying levels of naturally acquired immunity: a typical setting under which prevalence decays when $R_0 < 1$, and a setting in which subthreshold endemic equilibria exist. A qualitative comparison of the optimal control results under the first setting revealed that the optimal policy differs depending on whether the goal is to reduce total morbidity, or to reduce clinical infections. Furthermore, this comparison dictates that control programs should place less effort in vaccination as the level of NAI in a population, and as disease prevalence,

*Corresponding author, e-mail: olivia.f.prosper@dartmouth.edu

increase. In the second setting, we demonstrated that the optimal policy is able to confer long-term benefits with a ten-year control program by pushing the system into a new state where the disease-free equilibrium becomes the attracting equilibrium. While this result suggests that one can theoretically achieve long-term benefits with a short-term strategy, we illustrate that in this second setting, a small environmental change, or the introduction of new cases via immigration, places the population at high risk for a malaria epidemic.

KEYWORDS: mathematical model, differential equations, backward bifurcation, optimal control theory, leaky vaccines

1 Background

Due in part to the proliferation of artemisinin-resistant malaria, alternative strategies for controlling and reducing malaria burden have received much attention. Using multiple strategies simultaneously has proven remarkably effective at reducing malaria burden [10], and part of the recent reduction in malaria burden worldwide can be attributed to the integrated use of treatment and vector control strategies [25]. Vaccination is often cited as a promising tool for augmenting these integrated malaria control programs [20], though a malaria vaccine has yet to become available for large-scale use. Some vaccines are nearing certification, such as the RTS,S/AS01 vaccine being developed by GSK with a multinational consortium of government and non-governmental agencies [1]. The vaccines in development confer immunity and reduce the likelihood of transmission and infection through a variety of methods, and can be placed into one of three broad categories [17]: blood-stage targeting vaccines that increase the recovery rate of infected humans, gametic-stage targeting vaccines that reduce infectivity of humans to mosquitoes, and sporozoite-targeting vaccines (including RTS,S) that decrease susceptibility of humans to infection. Most malaria vaccines in development do not confer perfect immunity for the duration of immunity, however, and can be classified as leaky vaccines [18]. While leaky vaccines reduce an individuals infection risk, they do not prevent transmission entirely. For RTS,S, recent trials have suggested that vaccinated individuals are 40% less likely to become infected over a six month period, and are protected for roughly two years [23]. As a result, vaccines such as RTS,S alone are unlikely to eliminate malaria from areas with high malaria transmission. Balancing limited funding between vaccination and other controls to most efficiently reduce malaria burden is an important policy concern, and previous models have explored the possibility of using multiple controls concurrently [15]. Optimal control theory has been useful in addressing similar issues [19], and can be applied to optimize an objective (for example, reducing malaria deaths or overall malaria burden) by manipulation of controls [22], including vaccination and bednet usage. In regions of high malaria endemicity, immunity can occur naturally even in the absence of vaccination [16]. After an individual is exposed to malaria parasites repeatedly, infections no longer cause acute malaria and instead result in asymptomatic cases, though these individuals are still able to transmit parasites to mosquitoes [21]. While multiple

inoculations are required for this natural immunity to develop, people commonly receive enough inoculations to develop natural immunity to malaria before age 10 in areas with very high entomological inoculation rates; the exact mechanism for this phenomenon, however, remains unknown [21, 13]. Mathematical models have previously shown that naturally acquired immunity affects transmission dynamics, potentially influencing the utility of leaky vaccines [17]. In other disease systems, natural immunity has been shown to potentially cause a backward bifurcation [26], or a phenomenon where the disease can persist despite the basic reproductive number being under the typical critical threshold of unity. Backward bifurcations are important facets of disease systems, as backward bifurcations can lead to catastrophic reintroduction, and have been shown to be a property of some malaria models [9, 2]. Catastrophic reintroductions occur in settings where the introduction of a small number of cases when $R_0 < 1$ would not lead to reintroduction of the disease, but once R_0 increases above unity, a small reintroduction event causes a rapid move to an equilibrium with a high proportion of people infected [14]. Despite enthusiasm for malaria vaccine development, there is some skepticism about the ability of these leaky vaccines to reduce malaria burden, especially in areas with high rates of naturally acquired immunity [17]. If leaky vaccines reduce the amount of exposure individuals have to malaria, then vaccinated individuals may not develop natural immunity as quickly as without vaccination. Because infection remains possible for these vaccinated individuals, it is possible that they will be more likely to exhibit severe malaria when infected, as vaccination may prevent the development of natural immunity. Some modeling efforts have examined the impact of leaky vaccines on malaria burden in highly endemic areas, and previous models have suggested that in areas with very high rates of malaria transmission, using leaky vaccines may not reduce malaria burden appreciably, and may even cause increased rates of symptomatic malaria [17].

Because of the potentially complex interactions between immunity, vaccination, and malaria dynamics, predicting the outcome of a vaccination program and determining effective vaccination policy is an important concern. In this study, we determine the optimal vaccination policy in the presence and absence of naturally acquired immunity. We also determine the effect of naturally acquired immunity on the basic reproductive number and the endemic equilibrium of malaria prevalence. Under the Methods section, we first present a malaria vaccination model with naturally acquired immunity, followed by the extension of this model to include vaccination and bednet control efforts. A thorough analysis of the original model in the Results section reveals that naturally acquired immunity can render vaccination efforts counter-productive, and moreover, may lead to backward bifurcation at $R_0 = 1$. Lastly, using the optimal control construction, we present optimal vaccination and bed-net control strategies in populations with differing levels of naturally acquired immunity. The analytic and numerical analyses of our malaria vaccination model can help predict under which circumstances vaccination will be most effective at reducing malaria burden, and under which circumstances vaccination will be ineffective, or even counterproductive.

2 Methods

2.1 Model

We consider human and mosquito populations of constant sizes in a closed, homogeneous environment using a system of differential equations. The human population of size N is divided into five compartments: susceptible (S), infectious (I), recovered from clinical malaria (R), susceptible but partially protected (S_p), and individuals with partial protection who are infected and recovering (R_p). The infected mosquito population is modeled as a proportion z.

The system of ordinary differential equations in System (1) describes the disease dynamics in humans and mosquitoes. Initially, humans are susceptible (S). These susceptible individuals can either become vaccinated at a rate v and progress to S_p, or they can become infected at the rate βz, where β is the product of the ratio of mosquitoes to humans, the mosquito biting rate, and the mosquito-to-human-transmission efficiency. Once infected, the S-individual progresses to the infectious stage, I, and displays clinical symptoms. Individuals ultimately leave the I stage of the infection and enter R at a rate α, at which point they are no longer clinically ill, cannot move back to the clinical infection stage I, and are less infectious to mosquitoes. These asymptomatic, temporarily immune, partially infectious individuals have been previously incorporated into mathematical models of malaria [4, 8]. Recovering (R) individuals clear the infection at a rate r and either return to the susceptible, non-immune stage, S, or acquire partial immunity with probability q and become susceptible immune individuals (S_p). For simplicity, we assume that those who acquire partial temporary immunity through vaccination have the same protection as those who acquire it naturally. Subsequently, all individuals who acquire temporary immunity progress to the S_p stage regardless of the mechanism causing immunity. Vaccinated (or equivalently, partially immune), susceptible individuals will eventually either lose their immunity at a rate ω and return to the susceptible/non-immune class, or can become infected at a rate $\beta_p z$, where β_p is the transmission rate from mosquitoes to partially protected humans. Since immunity offers partial protection against malaria, we assume the inequality $\beta_p < \beta$. Individuals who become infected despite their acquired partial immunity progress to the R_p stage, where they are infectious with malaria, but are less infective to mosquitoes than individuals in the I stage. Eventually R_p infected individuals clear the infection and return to the S_p stage at a rate r_p.

The fraction of mosquitoes that are infected is denoted by z. As a result, $(1 - z)$ denotes the fraction of mosquitoes that are susceptible. The "I"-human-to-mosquito transmission rate is denoted by η_i, the "R"-human-to-mosquito transmission rate by η_r, and the "R_p"-human-to-mosquito transmission rate is denoted by η_p.

Finally, the human and mosquito natural mortality rates are denoted by μ and g respectively. To maintain a constant human population size, individuals are born into the susceptible class S at a rate μN, where $N = S + I + R + S_p + R_p$. Adding the first five equations in System (1), we indeed have that $N' = S' + I' + R' + S_p' + R_p' = 0$. This shows that N is constant, and in particular,

$N = S(0)+I(0)+R(0)+S_p(0)+R_p(0)$. Mosquito-borne disease models have mass action incidence terms when the human and mosquito states are both modeled as proportions of the total human and mosquito population, respectively, and when the transmission rate β (as described above) is the product of the ratio of mosquitoes to humans, biting-rate, and mosquito-to-human transmission efficiency [3, 6]. Consequently, modeling the human states in units of *number of individuals* and the mosquito states as *proportions* of the mosquito population yields incidence terms of the form $\beta z S$ for the rate of new human infections and $\left(\frac{\eta_i I + \eta_r R + \eta_p R_p}{N}\right)(1-z)$ for the rate at which new mosquito infections arise. All model state variables and parameters are summarized in Tables 1 and 2, respectively.

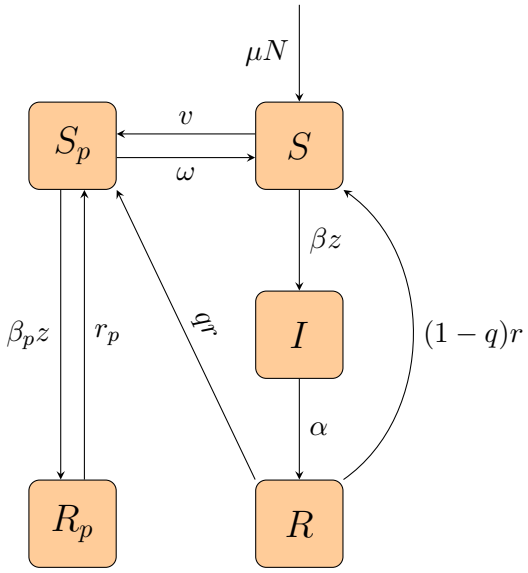

Figure 1: Human Dynamics Diagram

The description of the model can also be described mathematically as follows:

$$\begin{aligned}
S' &= \mu N - \beta z S + \omega S_p + (1-q) r R - (v+\mu) S \\
I' &= \beta z S - (\alpha + \mu) I \\
R' &= \alpha I - (r+\mu) R \\
S_p' &= r_p R_p + v S + q r R - (\beta_p z + \omega + \mu) S_p \\
R_p' &= \beta_p z S_p - (r_p + \mu) R_p \\
z' &= \left(\frac{\eta_i I + \eta_r R + \eta_p R_p}{N}\right)(1-z) - g z,
\end{aligned} \tag{1}$$

where $\beta_p = (1-e)\beta$, and e denotes the vaccine efficacy.

2.2 Optimal control of vaccination model

Malaria incurs significant economic costs for endemic regions, both incurring direct financial costs to the health system and costs associated with the reduced productivity of infected individuals. Resources for malaria control are also costly and limited. We used optimal control theory to determine how vaccination efforts and bed net distribution efforts may best be used to reduce disease burden, while simultaneously considering the cost of disease burden and implementation costs of the control program.

To determine the optimal control strategy, we reformulated System (1) to include vaccination and bednet usage. We redefine v to be the maximum possible vaccination rate and β, β_p, η_i, η_r, and η_p represent transmission parameters in the absence of bed-net efforts. The new variable $u_1(t)$ controls the vaccination rate, while the variable $u_2(t)$ controls the biting rate (and subsequently the transmission rates). These control variables are proportions, varying between zero and one. In this formulation of the model, v is replaced by $u_1 v$ and p is replaced by $(1-u_2)p$, where p is a transmission parameter ($p \in \{\beta_p, \eta_i, \eta_r, \eta_p\}$). When $u_1 = 0$, no vaccination occurs and when $u_1 = 1$, vaccination occurs at the maximum possible rate. Similarly, when $u_2 = 0$, there is no reduction in the transmission rates resulting from bed net efforts, while $u_2 = 1$ represents perfect protection from bed net use. Although several species of mosquito blood feed primarily at night, 100% bed net coverage will not eliminate malaria transmissions. To reflect the fact that bed nets are only effective at certain times of day, we restricted the range of u_2 to the interval [0,0.95]. Furthermore, if bed nets are not replaced or properly maintained, over time they deteriorate and begin to lose their efficacy as a result of repeated washing and natural wear-and-tear [5]. Thus, even if everyone in the population owns and uses a bed net, these nets may not be 100% effective; there is some effort required to maintain or replace bed nets over time. Subsequently, one may think of $u_2(t)$ as the effort placed into bed net maintenance at time t.

The modified model is as follows:

$$\begin{aligned}
S' &= \mu N - (1-u_2)\beta z S + \omega S_p + (1-q) r R - (u_1 v + \mu) S \\
I' &= (1-u_2)\beta z S - (\alpha + \mu) I \\
R' &= \alpha I - (r + \mu) R \\
S_p' &= r_p R_p + u_1 v S + q r R - ((1-u_2)\beta_p z + \omega + \mu) S_p \\
R_p' &= (1-u_2)\beta_p z S_p - (r_p + \mu) R_p \\
z' &= (1-u_2)\frac{\eta_i I + \eta_r R + \eta_p R_p}{N}(1-z) - g z.
\end{aligned} \tag{2}$$

Let the vector $f = (f_i)_{i=1}^6$ denote the right-hand side of the state system (2) and let $x = (x_i)_{i=1}^6$ denote the vector of state variables so that system (2) in vector notation is simply $\frac{dx}{dt} = f(x)$, with $x_1 = S, x_2 = I, x_3 = R, x_4 = S_p, x_5 = R_p, x_6 = z$ and $\frac{dx_i}{dt} = f_i(x)$.

As previously mentioned, implementing control measures incurs a cost. Our goal in applying optimal control theory to the malaria vaccination model was to determine a control strategy (using vaccines and bed net maintenance), that jointly minimizes the number of human infections and the cost of the program. Mathematically, the goal was to determine an optimal control pair $(u_1^*(t), u_2^*(t))$ that minimizes the cost functional

$$J = \int_0^T \left(w_1 I + w_2 R + w_3 R_p + w_4 u_1 v S + w_5 u_1^2 + w_6 u_2^2\right) \mathrm{d}t,$$

where the interval [0,T] represents the time interval over which the control program is conducted, and the w_i's are weights representing the relative costs of I, R, R_p and the control measures. Because there is always a limited stockpile of any vaccine, we wish to find a successful control strategy that aims to minimize the number of vaccines used over the duration of the program. The integral $\int_0^T u_1 v S \mathrm{d}t$ quantifies the total number of vaccines used during the program and has some relative cost w_4 associated with it. Thus, including this term in the objective function allowed us to take the limited availability of vaccines into consideration. To study the scenario where the quantity of vaccines is not a limitation imposed on the malaria control program, we may set w_4 to zero. Apart from limitations in vaccine availability, a control program should also take into consideration costs, including personnel and transportation, to distribute and maintain bed nets and administer vaccines. The term $w_5 u_1^2 + w_6 u_2^2$ in the objective function J incorporated these implementation costs to the control program.

Well known results from optimal control theory [27] allowed us to reformulate the problem of finding time-dependent control variables $u_1^*(t)$ and $u_2^*(t)$ that minimize J into the equivalent problem of minimizing the Hamiltonian

$$H = F + \sum_{i=1}^{6} \lambda_i f_i,$$

where F denotes the integrand of the objective functional J, and $\lambda := (\lambda_i)_{i=1}^6$ is the solution vector to the system of equations $\frac{d\lambda_i}{dt} = -\frac{dH}{dx_i}$ with the terminal condition $\lambda(T) = \vec{0}$. For our malaria model modified for vaccination and bednet usage (2), this system of differential equations, called

the adjoint system is the following:

$$\begin{aligned}
\lambda_1' &= -w_4u_1v + \lambda_1[(1-u_2)\beta z + u_1v + \mu] - \lambda_2(1-u_2)\beta z - \lambda_4 u_1 v \\
\lambda_2' &= -w_1 + \lambda_2(\alpha+\mu) - \lambda_3\alpha - \lambda_6(1-u_2)\frac{\eta_i}{N}(1-z) \\
\lambda_3' &= -w_2 - \lambda_1(1-q)r + \lambda_3(r+\mu) - \lambda_4 qr - \lambda_6(1-u_2)\frac{\eta_r}{N}(1-z) \\
\lambda_4' &= \lambda_1\omega + \lambda_4[(1-u_2)\beta_p z + \omega + \mu] - \lambda_5(1-u_2)\beta_p z \\
\lambda_5' &= -\omega_3 - \lambda_4 r_p + \lambda_5(r_p+\mu) - \lambda_6(1-u_2)\frac{\eta_p}{N}(1-z) \\
\lambda_6' &= (\lambda_1-\lambda_2)(1-u_2)\beta S + (\lambda_4-\lambda_5)(1-u_2)\beta_p S_p + \lambda_6\left[(1-u_2)\frac{\eta_i I + \eta_r R + \eta_p R_p}{N} + g\right],
\end{aligned}$$

with $\lambda(T) = \vec{0}$. The optimal control pair $(u_1^*(t), u_2^*(t))$ that solves the control problem is the pair of time-dependent functions that minimizes H. In other words, the pair must satisfy $\frac{\partial H}{\partial u_i} = 0$ and $\frac{\partial^2 H}{\partial u_i} > 0$, for $i = 1, 2$. Differentiating H with respect to the controls and solving for the u_i's, we obtain

$$\begin{aligned}
u_1^* &= min\left(max\left(0, \frac{\lambda_1^* - \lambda_4^* - w_4}{2w_5} v S^*\right), 1\right) \\
u_2^* &= min\left(max\left(0, \frac{(\lambda_2^* - \lambda_1^*)\beta S^* + (\lambda_5^* - \lambda_4^*)\beta_p S_p^*}{2w_6} z^* + \frac{\lambda_6^*}{2w_6}\frac{\eta_i I^* + \eta_r R^* + \eta_p R_p^*}{N}(1-z^*)\right), 0.95\right),
\end{aligned} \tag{3}$$

and $\frac{\partial^2 H}{\partial u_1^2} = 2w_5 > 0$ and $\frac{\partial^2 H}{\partial u_2} = 2w_6 > 0$. The notation $x^* = (S^*, I^*, R^*, S_p^*, R_p^*, z^*)$ is used to denote the solution to the state system corresponding to the optimal control pair (u_1^*, u_2^*).

State variables for resident of patch i	Description
S	Susceptible, non-immune individuals
I	Infectious, potentially clinically ill, non-immunes
R	Infectious asymptomatic non-immunes, with reduced infectivity
S_p	Susceptible, partially protected
R_p	Infected, partially-protected
z	Proportion of mosquitoes infected

Table 1

Parameter	Description
β	mosquito - to - S human transmission rate
β_p	mosquito - to - S_p human transmission rate
η_i	I - to - mosquito transmission rate
η_r	R - to - mosquito transmission rate
η_p	R_p - to - mosquito transmission rate
$1/\alpha$	Duration of initial infectious stage I
μ	Human natural mortality rate
r	R-stage human's parasite clearance rate
r_p	R_p-stage human's parasite clearance rate
q	Probability that an R individual acquires partial temporary immunity following parasite clearance
ω	Rate of loss of acquired immunity
v	Vaccination rate
m	ratio of mosquitoes to humans
a	biting rate
b	vector-to-human transmission efficiency
c	human-to-vector transmission efficiency
n	extrinsic incubation period

Table 2

3 Results and Discussion

3.1 Analytic results

To begin the study of the malaria vaccination model and the effects of partial, waning immunity, we present and analyze the basic reproduction number and equilibria of system (1).

3.1.1 The Basic Reproduction Number, R_0

The disease-free equilibrium (DFE) of the model is $(S_0^*, I_0^*, R_0^*, S_{p0}^*, R_{p0}^*, z_0^*) = \left(\frac{N(\omega+\mu)}{\omega+v+\mu}, 0, 0, \frac{Nv}{\omega+v+\mu}, 0, 0\right)$, where $N \equiv N(0)$ is constant. Following the Next Generation Approach (NGA) [12, 11], we arrive at the following expression for the basic reproduction number:

$$R_0 = \sqrt{\left(\frac{\eta_i}{\alpha+\mu} + \frac{\eta_r \alpha}{(\alpha+\mu)(r+\mu)}\right)\frac{\beta}{g} \cdot \frac{\omega+\mu}{\omega+v+\mu} + \frac{\eta_p}{r_p+\mu} \cdot \frac{\beta_p}{g} \cdot \frac{v}{\omega+v+\mu}}.$$

In epidemiology, the basic reproduction number is defined as the number of new infections arising from a single infected individual, in an otherwise fully susceptible population, during their lifespan as infectious. The square of our mathematically derived reproduction number can similarly be interpreted as the number of new mosquito infections arising from a single infectious mosquito. An intermediate host (humans, in our case) is needed to produce a new mosquito infection, and the contribution to new mosquito infections will depend on whether an infected mosquito takes a blood meal from a vaccinated human, or an unvaccinated human (note that at the disease-free equilibrium, there are no naturally immune individuals in the population). In fact, the first term under the square root represents the contribution to the reproduction number by a mosquito that takes a blood-meal from an unvaccinated individual; likewise, the second term represents the contribution by a mosquito that takes a blood-meal from a vaccinated individual. This interpretation is revealed by first noting that the fraction $\dfrac{\omega+\mu}{\omega+v+\mu}$ is the probability that a susceptible individual is not vaccinated, and $\dfrac{v}{\omega+v+\mu}$ is the probability a susceptible individual is vaccinated. Thus $\dfrac{\beta}{\gamma}\cdot\dfrac{\omega+\mu}{\omega+v+\mu}$ is the number of new infections arising in unvaccinated humans during the mosquito's lifespan as infectious, and $\dfrac{\beta_p}{\gamma}\cdot\dfrac{v}{\omega+v+\mu}$ is the number of new infections arising in vaccinated humans. To generate new *mosquito* infections, a non-vaccinated individual must transmit the infection to a healthy mosquito during his/her lifetime as infectious in stage I or stage R, or, a vaccinated individual must transmit the disease to a mosquito during their time as infectious in state R_p. Subsequently, $\dfrac{\beta}{g}\cdot\dfrac{\omega+\mu}{\omega+v+\mu}\cdot\dfrac{\eta_i}{\alpha+\mu}$ is the contribution to the reproduction number by a mosquito that takes a blood-meal from an unvaccinated individual, who then transmits malaria to a mosquito during their time as infectious in stage I. Similarly, $\dfrac{\beta}{g}\cdot\dfrac{\omega+\mu}{\omega+v+\mu}\cdot\dfrac{\eta_r\alpha}{(\alpha+\mu)(r+\mu)}$ is the contribution by a mosquito that takes a blood-meal from an unvaccinated individual who progresses to stage R, and transmits malaria to a mosquito during the time spent in the R stage. Finally, $\dfrac{\beta_p}{g}\cdot\dfrac{v}{\omega+v+\mu}\cdot\dfrac{\eta_p}{r_p+\mu}$ is the contribution to new mosquito infections arising from a mosquito that infects a vaccinated human, who then infects a mosquito during their time spent as infectious in stage R_p.

Typically, if $R_0<1$, the DFE is locally asymptotically stable (l.a.s.), and if $R_0>1$, the DFE is unstable. We will show, however, that this is not always the case for our malaria vaccination model. In this model, vaccination does not always reduce disease transmission metrics, as one might assume. Defining $A=\dfrac{\eta_i}{(\alpha+\mu)}+\dfrac{\eta_r\alpha}{(\alpha+\mu)(r+\mu)}$ and $B=\dfrac{\eta_p(1-e)}{r_p+\mu}$, if

(a) $A>B$, then R_0 is a decreasing function of v;

(b) $A=B$, then R_0 is constant in v;

(c) $A<B$, then R_0 is an increasing function of v.

This result (proved in Appendix A.1) has important implications for malaria control. In particular, it highlights that if $A < B$, introducing vaccination or increasing vaccination efforts may actually intensify disease transmission. When A and B are very close in value, increasing vaccination efforts may have little added benefit for a significant cost. Because of the formulation of A and B, knowledge about the human-to-mosquito transmission rates (η_i, η_r, η_p), the human disease progression and recovery rates (α, r, r_p), and the vaccine efficacy (e), in a given region, are necessary in our vaccination model to determine whether vaccination efforts will reduce the basic reproductive number.

These equations also allow us to consider ways of increasing the benefit of a vaccination program. For example, increasing the vaccine efficacy and decreasing the likelihood of transmission from vaccinated (but infected) humans (i.e. some portion of R_p-stage humans) to mosquitoes reduces B. On the other-hand, increasing recovery rates (r) of non-immune individuals, for example through improved treatment of asymptomatic individuals, decreases A, which may have negative effects on vaccination efforts.

3.1.2 Equilibria: multiplicity and stability

The equilibrium dynamics of the malaria vaccination model differed with and without NAI. A thorough analyses of these two cases reveals that in the absence of NAI ($q = 0$), the system exhibits a forward bifurcation at $R_0 = 1$, while a backward (subcritical) bifurcation at $R_0 = 1$ may occur in the case where $q \neq 0$. The result that when $q = 0$, the model has a unique endemic equilibrium when it exists, along with its proof (see Appendix A.2), implies that when $R_0 < 1$, the DFE is globally asymptotically stable (g.a.s.) if no R-stage individual gains temporary immunity to malaria, i.e. if $q = 0$. In other words, when $q = 0$, the model exhibits a forward transcritical bifurcation at $R_0 = 1$.

A useful result from center-manifold theory [7] allowed us to explore the dynamics of the model when $q \neq 0$ and establish the existence of more complicated dynamics. In particular, when $q \neq 0$, the model exhibits backward bifurcation if and only if

$$\left(\frac{\eta_i}{\alpha+\mu} + \frac{\eta_r \alpha}{(\alpha+\mu)(r+\mu)}\right)(r_1 - S_0^* r_6) + \frac{\eta_p(1-e)}{r_p+\mu}(r_2 - S_{p_0}^* r_6) > 0, \tag{4}$$

where r_6 is some positive constant, r_1 and r_2 are the solutions to the following system

$$\begin{aligned} -(v+\mu)r_1 + \omega r_2 + \left[\frac{(1-q)r\alpha}{(\alpha+\mu)(r+\mu)} - 1\right]\phi^* S_0^* r_6 = 0 \\ v r_1 - (\omega+\mu)r_2 + \left[\left(\frac{r_p}{r_p+\mu} - 1\right)(1-e)S_{p_0}^* + \frac{qr\alpha S_0^*}{(\alpha+\mu)(r+\mu)}\right]\phi^* r_6 = 0, \end{aligned} \tag{5}$$

and $\phi^* = \dfrac{g(\alpha+\mu)(r+\mu)(r_p+\mu)(\omega+v+\mu)}{\eta_i(r+\mu)(r_p+\mu)(\omega+\mu)+\eta_r\alpha(\omega+\mu)(r_p+\mu)+\eta_p(1-e)v(\alpha+\mu)(r+\mu)}$.

This result is proved in Appendix A.3. We can demonstrate numerically that there does, in fact, exist a region of parameter space for which inequality (4) holds. Thus, under certain parameterizations of model (1), the model exhibits backward bifurcation. An example of a backward bifurcation for our malaria vaccination model, using the parameter values in Table 5, is illustrated in Figure 2.

From the proof of equation (5) in Appendix A.3, we find that $r_1 < 0$. If $q = 0$, r_2 must also be negative, and consequently, inequality (4) is reversed, implying that backward bifurcation does not occur at $R_0 = 1$ when $q = 0$. Thus, the role of acquired immunity plays a critical role in the disease dynamics exhibited by this malaria vaccination model. Moreover, if $e = 1$, that is, immunity is perfect, then the left-hand side of equation (4) is negative and the bifurcation at $R_0 = 1$ is necessarily a forward bifurcation. This loss of backward bifurcation when either $q = 0$ or $e = 1$ indicates that naturally acquiring *partial* immunity to malaria is the driver of backward bifurcation. In the absence of vaccination ($v = 0$), we have that $r_2 > 0$, and moreover, it is still possible for backward bifurcation to occur. Thus, vaccination is not a driver of sub-threshold endemic equilibria in this model. However, $\psi > 0$ (where ψ denotes the left-hand side of 4) implies $B > A$, where A, B are defined as in equation (3.1.1); that is, R_0 an increasing function of the vaccination rate v is a necessary (although not sufficient) condition for backward bifurcation to occur. This suggests a potentially dangerous scenario when $R_0 < 1$ but malaria is still present in the population: increasing vaccination efforts, (which increases the reproduction number in this case), could push the disease dynamics from the region where the DFE is the local attractor into one where the larger endemic equilibrium (EE) is the attractor. This finding stresses that when R_0 is an increasing function of vaccination, other control measures (bednets, treatment, etc.) are necessary to bring R_0 below the critical threshold R_C. Another potentially dangerous scenario is one in which $R_C < R_0 < 1$ and a small fraction of the mosquito population is infected. Introducing new infected humans to the system, via migration for example, could again, push the system from a state where the DFE is the attractor, to one in which the EE is the attractor. This change arises from moving vertically in the bifurcation diagram. Likewise, environmental changes, such as land-use changes that are favorable for mosquito production, could push the system from a state where the DFE is locally stable to one where a positive EE is locally stable by increasing the reproduction number; in this scenario, the switch occurs by moving horizontally and to the right on the bifurcation diagram.

3.2 Numerical Analysis of backward bifurcation

In the previous section, we illustrated that the proportion of individuals who gain partial immunity (q) plays a critical role in the dynamics of the malaria model. In particular, if $q = 0$, the bifurcation at $R_0 = 1$ will be a forward bifurcation, and reducing R_0 below one is sufficient to stabilize the DFE; if $q \neq 0$, the possibility of sub-threshold endemic equilibria emerges, in which case reducing R_0

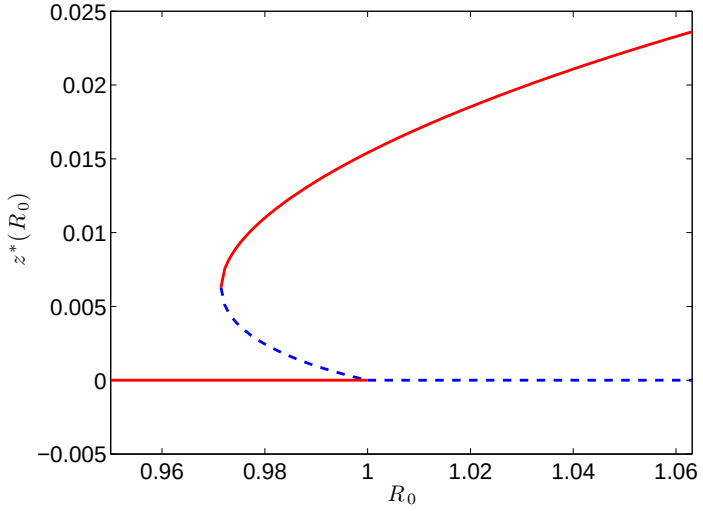

Figure 2: Illustration of Backward Bifurcation by plotting the equilibrium proportion of infected mosquitoes z^* as a function of R_0. The solid red curves denote the locally asymptotically stable equilibria; the dashed blue curves denote unstable equilibria. Parameter values in this simulation correspond to those in Table 5, and $v = 0$.

below unity may not be sufficient to eliminate malaria from the population. We also alluded to the fact that vaccination is not necessary for a backward bifurcation, despite the occurrence of backward bifurcation in many simple directly transmitted disease models with vaccination. Figure 2 illustrates the bifurcation diagram using the parameters in Table 5 in which there is no vaccination ($v = 0$). In this section, we explore potential consequences of partial temporary immunity, i.e. $q \neq 0$, with and without vaccination. Then, we illustrate numerically the relationship between $B - A$, ψ, and parameters that play important roles in determining the signs of these quantites to better understand the transmission characteristics most likely to lead to a subcritical equilbrium.

3.2.1 Existence of sub-threshold equilibria in the absence of vaccination

The presence of vaccination in our model is not necessary for the existence of backward bifurcation. This fact, which we demonstrated analytically in the previous section, can also be illustrated numerically by varying other parameters in the model and plotting the corresponding equilibria as a function of that parameter, or R_0. We first consider what happens as we vary ω, the waning immunity rate. Note that when $v = 0$, $R_0^2 = \left(\frac{\eta_i}{\alpha + \mu} + \frac{\eta_r \alpha}{(\alpha + \mu)(r + \mu)} \right) \frac{\beta}{g}$, and so the reproduction number no longer depends on parameters η_p, e, r_p, and ω. Despite the fact that R_0 is constant for any value of ω, we see in Figure 3, that multiple endemic equilibria exist for a particular R_0

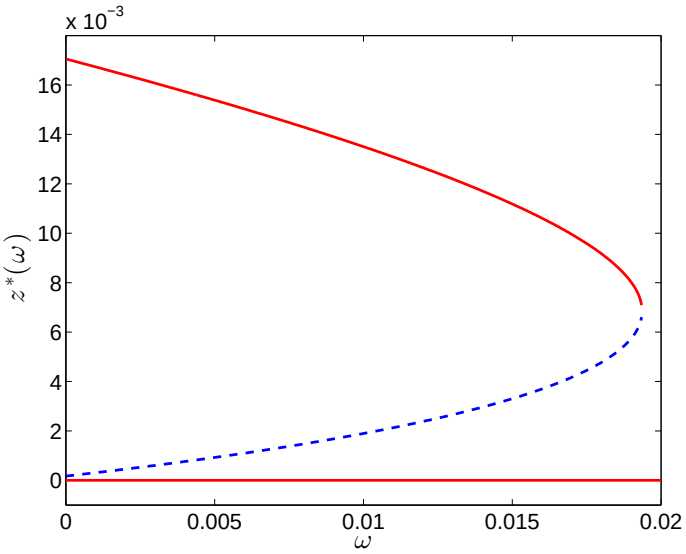

Figure 3: Backward Bifurcation with $v = 0$, varying ω. $R_0 = 0.9216$ for all ω in this example. The red solid curve denotes l.a.s. equilibria, the blue dashed curve denotes unstable equilibria. Parameter values in this simulation correspond to those in Table 5, except where otherwise stated.

value, and furthermore, for R_0 less than unity. In fact, two sub-threshold endemic equilibria appear when ω is small. For this parameterization of the model, the locally stable sub-threshold endemic equilibrium is largest when the naturally acquired partial immunity is permanent ($\omega = 0$). The same value of R_0 ($R_0 = 0.9216$ in Figure 3) is associated with wildly different equilibrium dynamics, depending on the value of ω. If $\omega \geq 0.0195$ the only equilibrium that exists is the disease free equilibrium. Otherwise, there exists a locally stable endemic equilibrium, an unstable positive equilibrium, and a locally stable DFE. When multiple equilibria exist, the disease outcome depends on the initial conditions of the system. This example, for which the same reproduction number can lead to very different long-term outcomes, stresses the limitations of using R_0 as the only measure of disease burden in a population.

3.3 ψ versus $B - A$

The numerical simulations support our conclusion in Section 3.1.2 that model parameterizations leading to backward bifurcation are a subset of parameterizations where R_0 increases with v. In other words, R_0 increasing with v is a necessary but not sufficient condition for a backwards bifurcation. Figure 4(a) illustrates that the region where $\psi > 0$ is a subset of the region where $B - A > 0$; Figures 4(b)-4(d) illlustrate how the bifurcation diagram changes as e increases. In particular, these figures demonstrate that backward bifurcation occurs for $e = 0.25$ and $e = 0.40$,

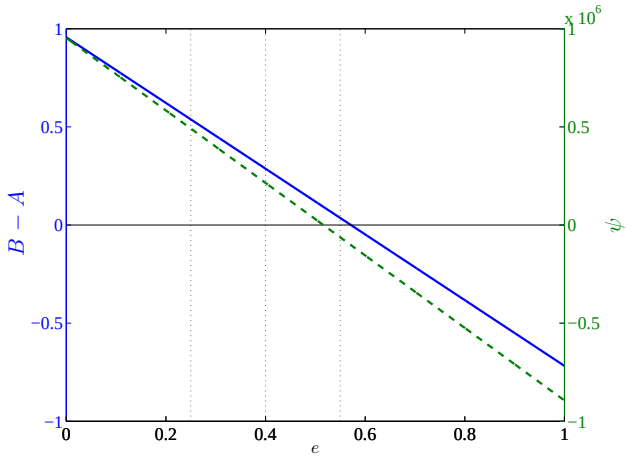

(a) $B - A$ and ψ plotted over values of e.

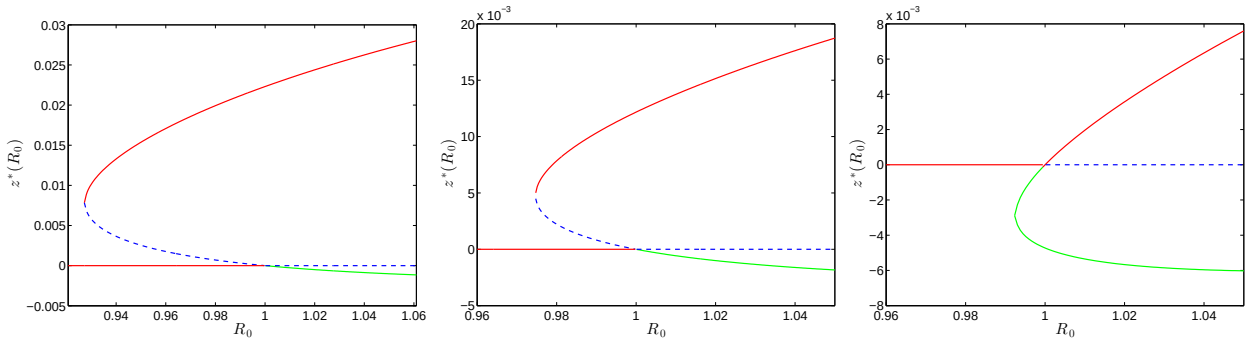

(b) $e = 0.25$ (c) $e = 0.40$ (d) $e = 0.55$

Figure 4: Subfigure (a) is a graph of $B - A$ and ψ as a function of the partial immunity efficacy e. The vertical dotted lines indicate where $e = 0.25, 0.40, 0.55$. Subfigures (b)-(d) illustrate three bifurcation diagrams corresponding to these different values of e. Red solid lines indicate locally asymptotically stable equilibria, blue-dashed lines indicate unstable equilibria, and green denotes biologically irrelevant equilibria. Parameter values in this simulation correspond to those in Table 5, except where otherwise stated.

that is, values of e for which $\psi > 0$. On the other hand, when $e = 0.55$, we have that $B - A > 0$, but $\psi < 0$, and therefore, the bifurcation at $R_0 = 1$ is in the forward direction. Furthermore, the critical threshold under which only the DFE exists, increases with increasing values of e.

Both the backward bifurcation and the cases where R_0 increased with v were more likely with changes to certain parameters. In particular, the numerical simulations showed that these phenomena are more likely to occur if immunity efficacy e is low. This result suggests that the presence of a backward bifurcation and the relationship between R_0 and v are dependent upon the relative contributions of each class of infectious individuals to transmission. If r_V is small relative to r, then temporarily immune individuals are infectious for a long period of time relative to nonimmune individuals. If the value of e is also low, then immune individuals are not significantly less susceptible than nonimmune individuals, and though immune individuals do not transmit malaria as easily as nonimmune individuals, they yield more new infections per infected individual than nonimmune individuals. Because naturally acquired immunity occurs when $q > 0$, then the introduction of malaria into a system increases the number of immune individuals ultimately, which reduces the threshold level of transmission necessary to drive the system to an endemic equilibrium. These results suggest that the presence of backward bifurcation depends, in part, on the relative contributions of immune and non-immune individuals to transmission, a hypothesis supported by Dushoff *et al* [14].

3.4 Results of optimal control

3.4.1 Optimal strategy in 'realistic' environment

We first present optimal solutions to the control problem over a time period of 120 months for a set of model parameters collected from the literature, largely from the Garki project [24]. These values have been used previously in studies of vaccine efficacy [17]. This set of parameters, listed in Table 3, leads to a forward bifurcation. In this section, we compare optimal malaria control strategies for four sets of weights, summarized in Table 4. We chose small values for the weights because we were interested in how the relative values of the weights affect the results rather than changes in their absolute value; using small values for the weights ensured convergence of the optimal control algorithm. The four weight sets reflect different goals that a malaria control program might have. Weight sets 2 and 4 weight only clinical infections (and therefore minimize only numbers of clinical infections), while weight sets 1 and 3 equally weight clinically infected individuals, recovering nonimmune individuals, and recovering immune individuals, seeking to minimize all infections. Weight sets 1 and 2 and weight sets 3 and 4 differ in that weight sets 3 and 4 much more heavily weigh the cost of infected individuals relative to the cost of bednets and vaccines.

Using the optimization method outlined in Appendix A.4, we optimized vaccination and bednet usage for $m \in \{2.5, 10, 30, 50, 70\}$ and $q \in \{0, 0.2, 0.4, 0.6, 0.8, 1\}$, where m is the ratio of the mosquito population size to the human population size in the region. Figure 6 summarizes the

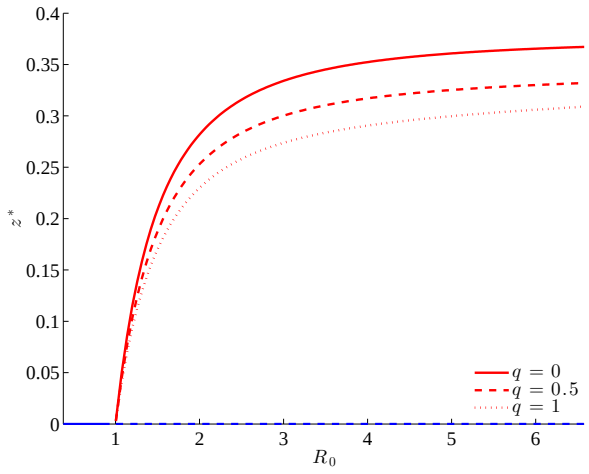

Figure 5: Bifurcation diagram for three different values of the natural immunity proportion q. The red curves represent the endemic equilibria as a function of R_0 and the blue line illustrates the disease-free equilibrium, which is stable for $R_0 < 1$ and unstable for $R_0 > 1$. Parameter values in this simulation correspond to those in Table 3, except where otherwise stated.

percent reduction in the number of human malaria infections, the number of vaccines administered, and the reduction in cost, respectively, resulting from the optimal control policy over a period of 10 years for these 120 settings with different weight sets. These bar charts illustrate that the optimal strategy when $m \in \{30, 50, 70\}$, is essentially to do nothing, as increasing vaccination or bednet coverage to a degree large enough to appreciably reduce malaria burden is prohibitively expensive. As vaccination and bednets do not greatly reduce malaria burden at high values of m, the optimal policy becomes significantly less advantageous when m is increased from 2.5 to 10. For example, for weight set 3, the percent reduction in malaria cases when the optimal strategy is employed decreases from roughly 11% to 2% when m increases from 2.5 to 10 (see row 3 in Figure 6(a)). This suggests that bednets and vaccines are most beneficial when the endemic equilibrium is small. Furthermore, it supports the result shown in the corresponding bifurcation diagram (see Figure 5): the equilibrium proportion of infected mosquitoes changes most dramatically when R_0 is close to one. In other words, the equilibrium of the proportion of infectious mosquitoes z is most sensitive to changes in R_0 when R_0 is close to (and greater than) 1. Thus, as m increases (and subsequently as R_0 increases), the equilibrium of the system becomes less sensitive to changes in the control variables. Similarly, for a fixed value of m, the efficacy of the optimal control program decreases as the natural immunity proportion q increases.

Figure 6 compares the reduction in the number of malaria cases (column 6(a)), the number of vaccines used (column 6(b)), and the reduction in cost (column 6(c)) under the optimal control policy for the 4 sets of weights, and for the different values of m and q. The first row of figures in

parameter	value	parameter	value
a	13.6875	ω	0.0833
b	0.0860	e	0.5200
c	0.470	μ	0.0011
g	6.0742	β	$mabe^{-gn}$
α	0.3285	β_p	$(1-e)\beta$
r	0.0359	η_i	ac
r_p	0.4076	η_r	$\sigma\eta_i$
n	0.3288	η_p	$\sigma\eta_i$
σ	0.5200	N	10,000

Table 3: Parameter set (in time unit of months) for optimal control problem in the forward bifurcating scenario. Values (with the exception of N) are taken from [17, 24]. The ratio of mosquitoes to humans m is varied in the numerical simulations.

set	w_1	w_2	w_3
1	10^{-7}	10^{-7}	10^{-7}
2	10^{-7}	0	0
3	$3 \cdot 10^{-7}$	$3 \cdot 10^{-7}$	$3 \cdot 10^{-7}$
4	$3 \cdot 10^{-7}$	0	0

Table 4: Four sets of weights used to numerically compute the optimal control solution $(u_1^*(t), u_2^*(t))$. In all sets of weights, the control variable weights are set to $w_4 = 10^{-7}$ and $w_5 = w_6 = 10^{-2}$.

Figure 6 presents the results for weight set 1, the second for weight set 2, and so on. Comparing the number of vaccines used to achieve a given percent cost reduction (Figure 6(c)), revealed that when the ratio of mosquitoes to humans m is 2.5, although many more vaccines (Figure 6(b)) are administered under this policy (roughly 9000 versus 2000 under weight set 3), the cost savings of the program is substantially more than when $m = 10$ (a 9% reduction versus a 2% reduction, roughly). As expected, increasing three-fold the cost associated with an infected individual yielded the greatest return in terms of both percent reduction in cases and relative reduction in cost.

A comparison of the qualitative dynamics of the optimal controls $u_1(t)$ and $u_2(t)$ for $m \in \{2.5, 10\}$, $q \in \{0, 0.2, 0.4, 0.6, 0.8, 1\}$, and for each of the four weight sets, allowed us to develop rules of thumb for how to implement bednets and vaccines in different environments, and to achieve different goals. The results for a subset of these scenarios are given in Figure 7. This figure illustrates the optimal control functions $u_1^*(t)$ and $u_2^*(t)$ over the 120 month control period and compares the disease dynamics without any malaria control to the disease dynamics under the optimal policies. In Figure 7 we present the results for weight sets 1 and 4 since these are the most directly comparable sets of weights, since $w_1 + w_2 + w_3 = 3 \cdot 10^{-7}$ in both cases. The general trend in the optimal vaccination strategy is to decrease efforts as the naturally acquired immunity proportion q increases.

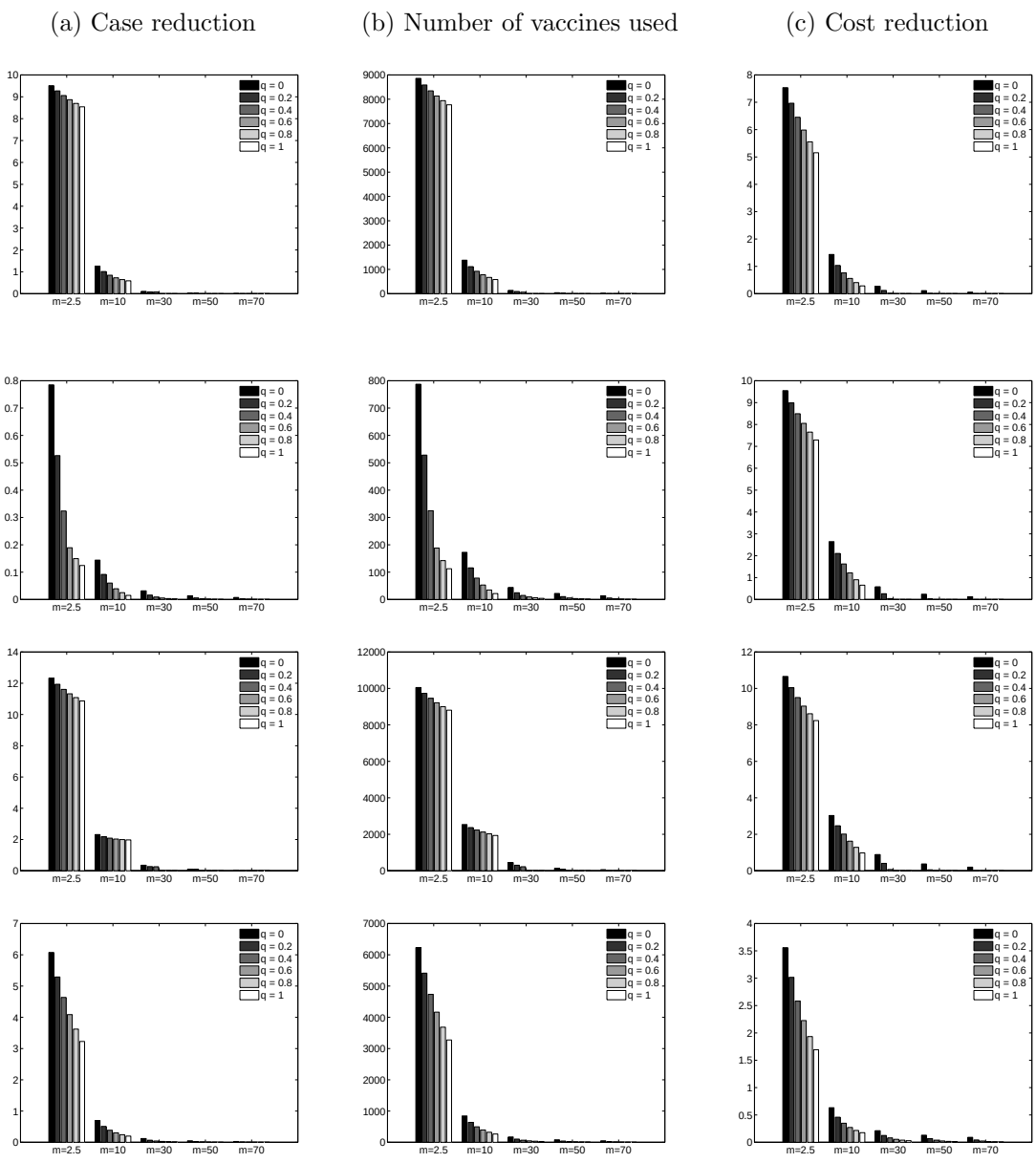

Figure 6: Barcharts illustrating the percent reduction in cases, vaccines used, and cost over a 10 year period as a result of the optimal control policy. The first row used weight set 1, the second row weight set 2, and so on. The percent reduction in cases is presented in column (a), the number of vaccines used in column (b), and the percent reduction in cost in column (c), for each of the four sets of weights. Parameter values in this simulation correspond to those in Table 3, except where otherwise stated.

Likewise, both controls decrease as m increases, across all scenarios. However, a comparison of the control strategies within each weight set and between weight sets does reveal some qualitatively different patterns.

First, we observed that the optimal control strategies across the 10 year period for weight sets 1 and 3, where the goal is to reduce total number of infections, are qualitatively very different from the optimal policies under weight sets 2 and 4, where the goal is to reduce the number of clinical infections. When the goal is to reduce the total number of infected individuals, the optimal vaccination strategy is a non-increasing function of time, decreasing to zero before the end of the control period (Figures 7(a)–7(b)). When $m = 10$, the optimal bednet control policy is one that is relatively constant during most of the control period, followed by a later increase in bed-net efforts to compensate for the decline in vaccination efforts. The level of compensation increases as q increases. This compensation phenomenon does not occur when $m = 2.5$. Perhaps more strikingly, when $m = 2.5$, the effort in bednet effort declines as q increases, whereas the opposite happens when $m = 10$. On the other hand, when the goal is to reduce the number of clinical infections, the optimal strategy for both controls is to ramp up efforts during the latter half of the control period (Figures 7(c)–7(d)). Vaccination and bednet efforts remain fairly constant during the first half of the control period, followed first by an increase in vaccination efforts, then by an increase in bednet efforts as the vaccination efforts begin decreasing to zero. The timing of these increases in effort is delayed as q and m increase. Thus, once again, we observed that bednet maintenance efforts should be increased to compensate for reductions in vaccination efforts. Unlike the results for the weight 1 and 3 scenarios, the optimal bednet efforts decreased not only with increasing m, but also with increasing q. To explore how a shorter control period may affect our results, we repeated the optimization for a two year period with $m = 2.5$ and for weight sets 1 and 4. For these select trials, we observed some similar qualitative patterns. However, to determine optimal control strategies for different time intervals, the numerical simulations should be repeated.

3.4.2 Optimal strategy in presence of sub-threshold endemic equilibrium

As discussed in Section 3.1, the possibility of backward bifurcation in our malaria model underscores the potential pitfalls of implementing a vaccination program without evaluating the current status of a particular population and environment: (1) reducing the reproduction number below unity may not be sufficient to eliminate malaria in the region, (2) vaccination may *increase* the reproduction number. However, importantly, the presence of backward bifurcation also opens up the opportunity to send the system towards the disease-free equilibrium with a control program of finite duration. If the bifurcation is forward at $R_0 = 1$, the only way to continue moving towards the disease-free equilibrium is to maintain R_0 below unity indefinitely by means of some control measure. If the bifurcation at $R_0 = 1$ is backwards, it becomes possible to "switch off" the control after some finite time, and still send the system towards the DFE. The goal of applying optimal control theory to the backward bifurcation setting was to determine whether the optimal vaccination and bednet coverage policy under a model parameterization leading to backward bifurcation is one that achieves this goal

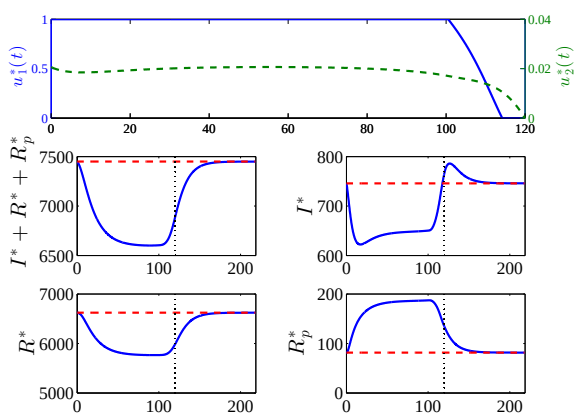

(a) Weight set 1, $m = 2.5$

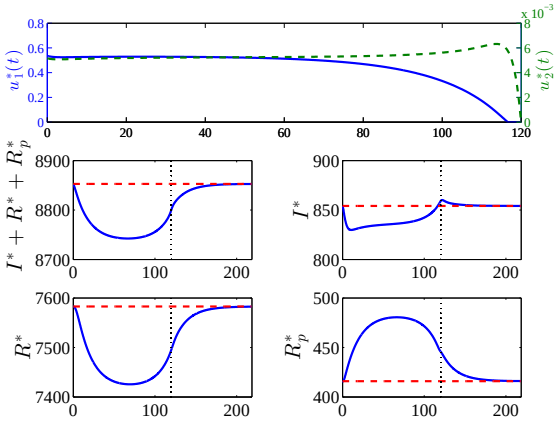

(b) Weight set 1, $m = 10$

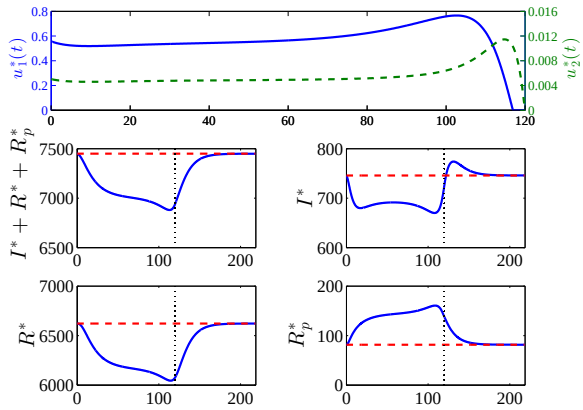

(c) Weight set 4, $m = 2.5$

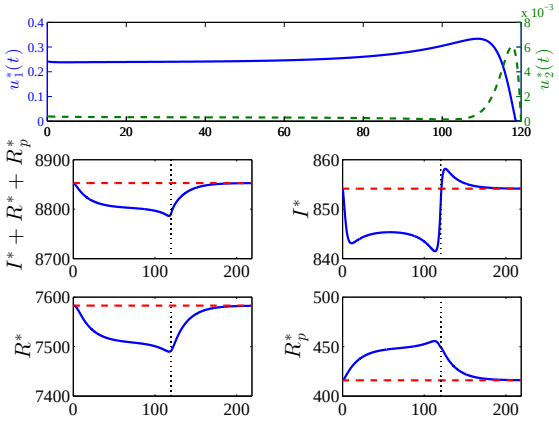

(d) Weight set 4, $m = 10$

Figure 7: Optimal control results in forward bifurcating scenario for weight sets 1 and 4, and $q = 0.2$. The figures illustrate the optimal control policies $u_1^*(t)$ and $u_2^*(t)$ and the infection dynamics with and without these optimal controls. The time scale along the horizontal axes of all figures is in months. The red dashed curves illustrate the endemic equilibrium in the absence of vaccination and bednet use. The blue curves in the infection dynamics illustrate the disease dynamics under the optimal control policy. The vertical dashed line indicates the end of the 10 year control period (120 months). In the left column, the ratio of mosquitoes to humans m is 2.5, in the right column, $m = 10$. The first row of figures illustrates results for weight set 1; the second row corresponds to weight set 4. Parameter values in this simulation correspond to those in Table 3, except where otherwise stated.

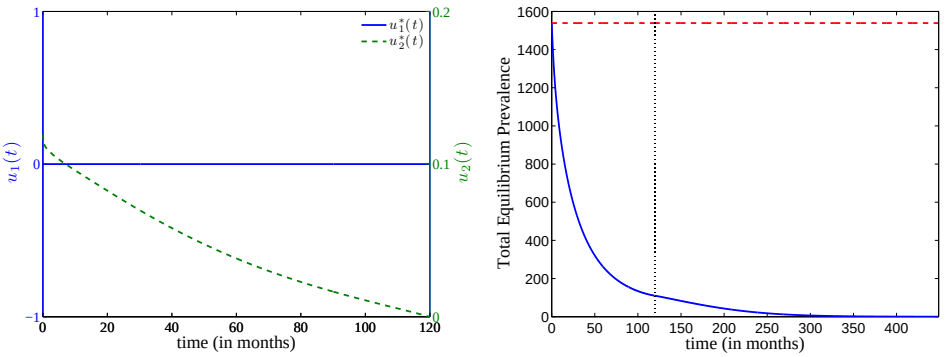

(a) (b)

Figure 8: (a) Optimal control policy under a backward bifurcation scenario. Under the optimal policy, the control function $u_1^*(t)$, which controls the vaccination rate, is constantly zero; the initial bednet coverage $u_2^*(t)$ is 12%, gradually decreasing over the 120 month period to 0% coverage. (b) Disease dynamics in humans under the optimal control policy. The vertical dashed line indicates the end of the 120 month control period. The red dashed line is the total equilibrium number of infected in the absence of control ($u_1(t) = u_2(t) = 0$). The solid blue lines illustrate the total number of infected individuals over time with the optimal policy up to month 120 and with no control thereafter. Parameter values in this simulation correspond to those in Table 5, except where otherwise stated.

of stabilizing the DFE even after the control period ends. Using the parameter values listed in Table 5, which led to backward bifurcation, and using weight set 1, we numerically computed the optimal control solution. Consistent with our previous analyses that the presence of backward bifurcation implies that R_0 is an increasing function of the vaccination rate, the numerically computed optimal solution dictates that we should not vaccinate at any time; that is, $u_1^*(t) = 0$ for all t. Meanwhile, the optimal bednet coverage $u_2^*(t)$ is initially 12% and decreases gradually to 0% coverage by the end of the 120 month control period (Figure 8).

Figure 8(b) compares the disease dynamics when $u_1(t) = u_2(t) = 0$ (red-dashed line) to the disease dynamics under the optimal control policy (blue solid line). The vertical black dotted line designates the end of the control period. Although bednet coverage is 0% from month 120 onwards, we can see in Figure 8(b) that the number of malaria infections still tends towards zero. Thus, the optimal policy not only minimizes infections and cost during the control period, but also has long-term benefits. Figure 9 superimposes the trajectory of the proportion of infected mosquitoes z under the optimal policy onto the bifurcation diagram for the system under this parameterization. The proportion of infected mosquitoes at equilibrium in the absence of any bednet efforts is indicated with a solid black circle; the start of the trajectory of z under the optimal policy is indicated with a solid black square. From this figure, we can see that the optimal

control policy instantaneously moves the system from the black circle horizontally to the black square by reducing R_0 to approximately 0.85. This reduction in R_0 (by means of increasing u_2) causes the proportion of infected mosquitoes z to decrease. The optimal policy gradually decreases bednet coverage $u_2^*(t)$ in such a way that although R_0 increases, $z(t)$ decreases sufficiently so as to stay in the region where the DFE is the attracting equilibrium. This makes it possible to stop controls completely after a finite period of time, while still sending the system towards the disease-free equilibrium.

4 Conclusions

Vaccines have played a fundamental role in the control, and, in some cases, eradication of infectious disease. Most vaccines are considered leaky vaccines and do not provide perfect protection, but are effective enough to provide herd immunity for a population. These successes give hope that malaria vaccines, such as RTS,S, will be an effective way to combat this dangerous disease that has eluded control efforts for so long. Our malaria vaccination model presented here, however, emphasizes the importance of obtaining high vaccine efficacy and prudent vaccination policy, particularly in populations with an existing level of naturally acquired immunity. Analysis of the model basic reproduction number revealed that certain environments and control policies may in fact render the vaccine harmful to the goal of reducing overall disease burden. In particular, if non-immune, infected individuals are treated more readily than partially immune infected individuals, the likelihood that malaria transmission will rise with increased vaccination efforts increases. This scenario is plausible, as partially immune individuals tend to have less severe symptoms when infected with malaria, and are therefore less likely to be treated. These results, then, suggest that we may be able to increase the efficacy of a vaccination program at the population level by actively searching for, and treating, asymptomatic infections.

Subsequently, our result that backward bifurcation can only occur if R_0 is an increasing function of vaccination indicates that active case detection may help to avoid the potentially dangerous scenario of backward bifurcation. By treating asymptomatic infected individuals, the infectious period for immune individuals will be reduced, making a backward bifurcation less likely. The presence of backward bifurcation at $R_0 = 1$ is problematic in part because the usual goal of reducing the reproduction number below unity is insufficient in this setting. Instead, to guarantee that the disease-free equilibrium is the only equilibrium, control programs must strive to push R_0 below some smaller critical threshold R_C. Perhaps more importantly, however, backward bifurcation can give rise to large-scale malaria epidemics as a result of small changes in the environment and migration. For example, a small change in climate, or slight reduction in existing control efforts, can increase the reproduction number by making the environment more suitable for mosquito production or parasite development, causing the potential for a catastrophic reintroduction of malaria [14]. Both of these changes, that is, small changes in R_0 and small changes in prevalence, can move the system from the disease-free equilibrium region of attraction, to a large endemic equilibrium region

of attraction, causing devastating outbreaks.

Investigating optimal vaccination and bed net maintenance strategies over a 10-year period allowed us to gain a qualitative understanding of how these two controls should be used in tandem, and how they should be used in different malaria endemic settings. First, we considered the more common scenario where the bifurcation at $R_0 = 1$ is a forward bifurcation. In general, we found that as the ratio of mosquitoes to humans increases, which in turn increases overall prevalence, implementing a vaccination and bed net control policy becomes much costlier and less effective. In regions of very high malaria prevalence, other methods of malaria control may be necessary; once prevalence is sufficiently reduced, vaccination may become a viable option for malaria control. We also found that as the proportion of the population with NAI is increased, less effort should be placed in vaccination efforts.

The optimal policies were qualitatively different depending on whether the goal was to reduce clinical infections or reduce total disease prevalence. To reduce total prevalence, the best vaccination strategy is to begin the control period with a higher rate of vaccination and gradually decrease this effort over time. When initial burden is high, bed net efforts should increase as vaccination efforts begin decreasing. On the other hand, if the goal is to reduce clinical cases of malaria, both vaccination and bed net efforts remain at some constant level for the first half of the control period, followed by a surge in vaccination efforts; as vaccination efforts decline to zero following this surge, bed net efforts should increase to compensate.

If a backward bifurcation exists, we found that vaccination should not be part of the control program; this result is consistent with our conclusions that R_0 increasing with vaccination is a necessary, although not sufficient, condition for backward bifurcation to arise. The optimal solution instead consists of steadily decreasing bed net efforts over time. The optimal policy takes advantage of the backward bifurcation at $R_0 = 1$ by moving the system from the larger endemic equilibrium to the region where the disease-free equilibrium is the attractor within the ten-year control period. By pushing the system to this region of the bifurcation diagram, the system is able to move towards the disease-free equilibrium even after control measures have been lifted - a result that is not possible in the forward bifurcation scenario. Although theoretically it is possible to take advantage of the backward bifurcation to impart long-term benefits from a short-term control strategy, it is important to always keep in mind the caveat that a small environmental change or a small reintroduction event could easily move the system back into the endemic equilibrium attracting region. This means that although the system is tending towards elimination beyond the control period, the likelihood of an epidemic event is high.

The natural step in furthering our understanding of the interaction between leaky vaccines and NAI is to extend our current model to allow the level of naturally acquired immunity to change with changes in malaria prevalence. Our model as is does not consider that vaccines are likely to, over time, reduce NAI levels in a population. According to our analyses, if the time scale on which NAI changes as a result of vaccine use is fast, this should have a dramatic impact on the optimal control results; vaccines would become more effective at the population level as NAI decreases as a

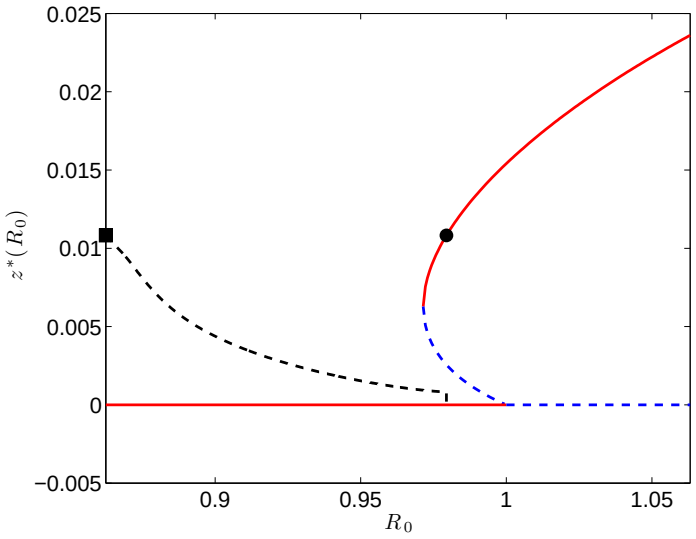

Figure 9: The black, dashed curve illustrates the trajectory of the proportion of mosquitoes infected $z(t)$ during, and several months beyond, the control period, superimposed on the bifurcation diagram for the system. The beginning of the trajectory is marked with a black square. The equilibria of the bifurcation diagram are illustrated in red and blue. The red, solid curves represent the locally asymptotically stable equilibria, while the blue, dashed curves represent the unstable equilibria as a function of R_0. The bifurcation parameter used in this illustration was β. The black dot represents the location of the equilibrium value z^* prior to any control policy (that is, $u_1 = u_2 = 0$). Parameter values in this simulation correspond to those in Table 5, except where otherwise stated.

consequence of vaccination. If on the other hand, levels of NAI change relatively slowly, our model may be a reasonable approximation over short time intervals.

With a relatively simple malaria model, we have demonstrated the importance of understanding the impact of NAI and leaky vaccines on the efficacy of a malaria vaccination program and highlighted that such a program is unlikely to be "one size fits all". How leaky vaccines are distributed should be region specific, depending not only on environmental characteristics that lead to different malaria-relevant parameters, but also on the underlying level of natural immunity in the population.

parameter	value	parameter	value
a	3.1938	ω	0.0563
b	0.1000	e	0.3000
c	0.2140	μ	0.0013
g	5.0796	β	$mabe^{-gn}$
α	4.3452	β_p	$(1-e)\beta$
r	0.6083	η_i	ac
r_p	0.2028	η_r	$\sigma\eta_i$
n	0.3288	η_p	$\sigma\eta_i$
σ	0.5000	N	10,000

Table 5: Parameter set (in time unit of months) for optimal control problem in the backward bifurcating scenario. Note: parameter values for backward bifurcation setting are not taken from the literature.

Competing Interests

The authors declare that they have no competing interests.

Acknowledgements

OP and NR were partially supported by the National Science Foundation under Grant No. 0801544 in the Quantitative Spatial Ecology, Evolution and Environment Program at the University of Florida, as well as the Emerging Pathogens Institute at the University of Florida. MM is in part supported by grant DMS-1220342. The authors acknowledge DL Smith for valuable discussions at the beginning of this project. Finally, we thank the anonymous reviewers for their thoughtful feedback.

A Appendix

A.1 Proof that R_0 can be decreasing, constant, or increasing with v

First, $R_0^2 = A\frac{\omega+\mu}{\omega+v+\mu}\cdot\frac{\beta}{g} + B\frac{v}{\omega+v+\mu}\cdot\frac{\beta}{g}$. Thinking of R_0 as a function of v and differentiating R_0^2 with respect to v, we have

$$2R_0\frac{dR_0}{dv} = \frac{\omega+\mu}{(\omega+v+\mu)^2}\cdot\frac{\beta}{g}(B-A),$$

and the conclusion is straightforward.

A.2 Proof that there is a unique endemic equilibrium when $q = 0$, $R_0 > 1$.

Suppose $z^* \neq 0$. From our system of differential equations , we find that

$$S^* = \frac{\mu N + \omega S_p^* + r R^*}{\beta z^* + v + \mu} \tag{6}$$

$$I^* = \frac{\beta z^* S^*}{\alpha + \mu} \tag{7}$$

$$R^* = \frac{\alpha \beta z^* S^*}{(\alpha + \mu)(r + \mu)} \tag{8}$$

$$S_p^* = \frac{r_p R_p^* + v S^*}{(1-e)\beta z^* + \omega + \mu} \tag{9}$$

$$R_p^* = \frac{(1-e)\beta z^* S_p^*}{r_p + \mu} \tag{10}$$

Substituting Equation (9) into Equation (10) and solving for R_p^*, we obtain

$$R_p^* = \frac{(1-e)\beta v z^* S^*}{(r_p + \mu)\left[(1-e)\beta z^* + \omega + \mu\right] - r_p(1-e)\beta z^*}.$$

Let $f_1(z^*) = \dfrac{r_p(1-e)\beta z^*}{(r_p + \mu)\left[(1-e)\beta z^* + \omega + \mu\right]}$. From Equations (9-10), we can rewrite S_p^*:

$$S_p^* = \frac{v S^*}{(1 - f_1(z^*))((1-e)\beta z^* + \omega + \mu)}. \tag{11}$$

Using Equations (6), (8), and (11), we can now write S^* in terms of z^* alone:

$$S^* = \frac{\mu N}{(1 - f_2(z^*))(\beta z^* + v + \mu)},$$

where $f_2(z^*) = \dfrac{\omega v}{(1 - f_1(z^*))\left[(1-e)\beta z^* + \omega + \mu\right](\beta z^* + v + \mu)} + \dfrac{r\alpha\beta z^*}{(\alpha + \mu)(r + \mu)(\beta z^* + v + \mu)}$. Substituting this expression into the equation for $z' = 0$, we obtain an equation in z^*:

$$\frac{\beta\mu(1 - z^*)}{(1 - f_2(z^*))(\beta z^* + v + \mu)}\left[\frac{\eta_i}{\alpha + \mu} + \frac{\eta_r \alpha}{(\alpha + \mu)(r + \mu)} + \frac{\eta_p(1-e)v}{(r_p + \mu)\left[(1-e)\beta z^* + \omega + \mu - r_p(1-e)\beta z^*\right]}\right] = g \tag{12}$$

Let $F(z^*)$ denote the left-hand side of Equation (12). $F(0) = R_0 g$. So, $R_0 > 1$ implies $F(0) > g$. On the other hand, $F(1) = 0 < g$. Thus, a solution to Equation (12) exists. To show that Equation (12) has, in fact, a unique solution, we will show that $F(z^*)$ is a monotonically decreasing function.

The term in brackets in Equation (12) is clearly a decreasing function of z^*. Furthermore, $(1 - f_1(z^*))\left[(1-e)\beta z^* + \omega + \mu\right] = \omega + \mu + \dfrac{\mu(1-e)\beta z^*}{r_p + \mu}$ implies that

$$\begin{aligned}
(1 - f_2(z^*))(\beta z^* + v + \mu) &= \beta z^* + v + \mu - \frac{\omega v}{(1 - f_1(z^*))\left[(1-e)\beta z^* + \omega + \mu\right]} - \frac{r\alpha\beta z^*}{(\alpha+\mu)(r+\mu)} \\
&= \beta z^* + v + \mu - \frac{\omega v(r_p + \mu)}{(\omega+\mu)(r_p+\mu) + \mu(1-e)\beta z^*} - \frac{r\alpha\beta z^*}{(\alpha+\mu)(r+\mu)} \\
&= \beta z^* \left(1 - \frac{r\alpha}{(\alpha+\mu)(r+\mu)}\right) + v + \mu - \frac{\omega v(r_p+\mu)}{(\omega+\mu)(r_p+\mu) + \mu(1-e)\beta z^*}.
\end{aligned}$$

Thus, $(1 - f_2(z^*))(\beta z^* + v + \mu)$ is an increasing function of z^*, and so we have that $\dfrac{\beta\mu(1-z^*)}{(1 - f_2(z^*))(\beta z^* + v + \mu)}$ is monotonically decreasing in z^*. So, $F(z^*)$ is a monotonically decreasing function, while the right hand side is constant in z^*. Therefore, Equation (12) has a unique solution $z^* = \hat{z}$.

A.3 Proof of conditions for backward bifurcation

We first refer to the following useful result based on general center manifold theory, and the remark that follows:

Theorem A.3.1. *(Castillo-Chavez and Song)*

Let $\frac{dx}{dt} = f(x, \phi)$ refer to a general system of ordinary differential equations, where $f : \mathbf{R}^n \times \mathbf{R} \to \mathbf{R}^n$, $f \in \mathbf{C}^2(\mathbf{R}^n \times \mathbf{R})$, and ϕ is a parameter. Without loss of generality, let 0 be an equilibrium of the system so that $f(0, \phi) = 0$ for all ϕ. Assume

(1) $A = D_x f(0, 0)$, i.e. the Jacobian of the system evaluated at the zero equilibrium, with $\phi = 0$. Zero is a simple eigenvalue of A and all other eigenvalues of A have negative real parts;

(2) Matrix A has a nonnegative right eigenvector w and a left eigenvector v corresponding to the zero eigenvalue.

Let f_k be the k^{th} component of f and

$$a = \sum_{k,i,j=1}^{n} v_k w_i w_j \frac{\partial^2 f_k}{\partial x_i \partial x_j}(0,0) \tag{13}$$

$$b = \sum_{k,i=1}^{n} v_k w_i \frac{\partial^2 f_k}{\partial x_i \partial \phi}(0,0). \tag{14}$$

Then, the local dynamics of the system are completely determined by the signs of a and b. In particular, if $a, b > 0$, the bifurcation at $\phi = 0$ is subcritical (i.e. backward).

Remark A.3.2. *The condition in assumption (2) of Theorem A.3.1 that the right eigenvector w be positive is not necessary. In fact, if x_0 denotes the equilibrium, we only need that $w(j) > 0$ whenever $x_0(j) = 0$. If $x_0(j) > 0$, then $w(j)$ need not be positive.*

Proof. Denote the vector of state variables in our model by $x = (S, S_p, I, R_p, R, z)^T$ Let x_0 denote the DFE of system (1) with the ordering designated by the vector x.

Let $\phi = \beta$. Then,

$$D_x f(U_0, \phi) = \begin{pmatrix} A_1 & A_2(\phi) \\ 0 & A_3(\phi) \end{pmatrix}, \tag{15}$$

where

$$A_1 = \begin{pmatrix} -(v+\mu) & \omega \\ v & -(\omega+\mu) \end{pmatrix}, A_2(\phi) = \begin{pmatrix} 0 & 0 & (1-q)r & -\phi S_0^* \\ 0 & r_p & qr & -(1-e)\phi S_{p0}^* \end{pmatrix}, \text{ and}$$

$$A_3(\phi) = \begin{pmatrix} -(\alpha+\mu) & 0 & 0 & \phi S_0^* \\ 0 & -(r_p+\mu) & 0 & (1-e)\phi S_{p0}^* \\ \alpha & 0 & -(r+\mu) & 0 \\ \frac{\eta_i}{N_0^*} & \frac{\eta_p}{N_0^*} & \frac{\eta_r}{N_0^*} & -g \end{pmatrix}.$$

The eigenvalues of the block triangular matrix $D_x f(U_0, \phi)$ are precisely the eigenvalues of A_1 and $A_3(\phi)$. A_1 has negative trace and positive determinant ($det(A_1) = \mu(\omega + v + \mu) > 0$), hence all eigenvalues of A_1 have negative real part. $det(A_3 - \lambda I)$ is of the form $p(\lambda) = a_0 + a_1\lambda + a_2\lambda^2 + a_3\lambda^3 + \lambda^4$.

$$\begin{aligned} p(\lambda) = &-\frac{\eta_i}{N}(r_p+\mu+\lambda)(r+\mu+\lambda)\phi^* S_0^* - \frac{\eta_p}{N}(r+\mu+\lambda)(\alpha+\mu+\lambda)(1-e)\phi^* S_{p0}^* \\ &- \frac{\eta_r \alpha}{N}(r_p+\mu+\lambda)\phi^* S_0^* + (g+\lambda)(\alpha+\mu+\lambda)(r_p+\mu+\lambda)(r+\mu+\lambda) \end{aligned}$$

A little algebra reveals that $a_0 = 0$ when $\phi = \phi^*$, and so, zero is an eigenvalue of $A_3(\phi^*)$. Note that it is clear that zero must be an eigenvalue because $\phi = \phi^*$ precisely when $R_0 = 1$. Furthermore, a_1 can be written as follows, and easily seen to be positive:

$$\begin{aligned}
a_1 =& g(\alpha+\mu)(r_p+\mu)\left[1-\left(\frac{\eta_i S_0^*}{N(\alpha+\mu)}+\frac{\eta_p(1-e)(S_p^*)_0}{N(r_p+\mu)}\right)\frac{\phi^*}{g}\right] \\
&+ g(\alpha+\mu)(r+\mu)\left[1-\frac{\eta_i S_0^*}{N(\alpha+\mu)}\frac{\phi^*}{g}\right] \\
&+ g(r_p+\mu)(r+\mu)\left[1-\frac{\eta_p(1-e)S_{p0}^*}{N(r_p+\mu)}\frac{\phi^*}{g}\right] + (\alpha+\mu)(r+\mu)(r_p+\mu) \\
>& \left(g(\alpha+\mu)(r_p+\mu)+g(\alpha+\mu)(r+\mu)+g(r_p+\mu)(r+\mu)\right)\left(1-R_0^2(\phi^*)\right) \\
&+ (\alpha+\mu)(r+\mu)(r_p+\mu) \\
=& (\alpha+\mu)(r+\mu)(r_p+\mu) > 0.
\end{aligned}$$

Because $a_0 = 0$ and a_1 is positive, $p(\lambda)$ has precisely one zero root; in other words, $A_3(\phi^*)$ has a simple zero root. The remaining coefficients a_2 and a_3 are also positive, and so by Descartes' Rule of Signs, $p(\lambda)$ has no positive real roots.

To show that $p(\lambda)$ has no complex roots with positive real part, we assume, by way of contradiction, that there exists $s \geq 0$ and $t \neq 0$ (both real) such that $\lambda = s + it$ is a root of $p(\lambda)$. Note that $p(\lambda) = (g + \lambda - L(\lambda))(\alpha+\mu+\lambda)(r_p+\mu+\lambda)(r+\mu+\lambda)$, where

$$L(\lambda) = \frac{\eta_i \phi^* S_0^*}{N(\alpha+\mu+\lambda)} + \frac{\eta_p(1-e)\phi^* S_{p0}^*}{N(r_p+\mu+\lambda)} + \frac{\eta_r \alpha \phi^* S_0^*}{N(\alpha+\mu+\lambda)(r+\mu+\lambda)}.$$

Then, $p(s+it) = 0$ if and only if $L(s+it) = g + s + it$. Note that $|x+s+it| > x+s$ for any $x > 0$. Thus,

$$\begin{aligned}
|L(s+it)| &\leq \frac{\eta_i \phi^* S_0^*}{N|\alpha+\mu+\lambda|} + \frac{\eta_p(1-e)\phi^* S_{p0}^*}{N|r_p+\mu+\lambda|} + \frac{\eta_r \alpha \phi^* S_0^*}{N|\alpha+\mu+\lambda||r+\mu+\lambda|} \\
&< \frac{\eta_i \phi^* S_0^*}{N(\alpha+\mu+s)} + \frac{\eta_p(1-e)\phi^* S_{p0}^*}{N(r_p+\mu+s)} + \frac{\eta_r \alpha \phi^* S_0^*}{N(\alpha+\mu+s)(r+\mu+s)} \\
&= L(s) = g + s.
\end{aligned}$$

So, $|L(s+it)| < g + s$. On the other hand, $|L(s+it)| = |g+s+it| > g+s$, which contradicts the previous inequality. Therefore, if $\lambda = s + it$ for some $t \neq 0$, then $s < 0$. That is, any complex roots of $p(\lambda)$ have negative real part.

To summarize these conclusions, $A_3(\phi^*)$ has a simple zero eigenvalue and all other eigenvalues have negative real part. Therefore, assumption (1) in Theorem A.3.1 holds for our system.

We denote the left and right eigenvectors associated with the zero eigenvalue by l and r, respectively. The component r_6 is arbitrary and may be chosen positive. The first and second components of r are the solutions to system (5). The remaining components of the right eigenvector are given by

$$\begin{aligned} r_3 &= \frac{\phi^* S_0^*}{\alpha+\mu} r_6 \\ r_4 &= \frac{\phi^*(1-e) S_{p0}^*}{r_p+\mu} r_6 \\ r_5 &= \frac{\alpha\phi^* S_0^*}{(\alpha+\mu)(r+\mu)} r_6. \end{aligned}$$

Solving for r_2 in the second equation (in terms of r_1) of system (5) and plugging into the first equation, we obtain

$$\begin{aligned} \frac{\mu(\omega+v+\mu)}{\omega+\mu} r_1 =& \frac{\omega}{\omega+\mu}\left(\frac{r_p}{r_p+\mu}-1\right)(1-e)S_{p0}^*\phi^* r_6 \\ &+ \left[\frac{\omega}{\omega+\mu}\cdot\frac{qr\alpha}{(\alpha+\mu)(r+\mu)} + \frac{(1-q)r\alpha}{(\alpha+\mu)(r+\mu)} - 1\right]\phi^* S_0^* r_6. \end{aligned} \tag{16}$$

Each term on the right hand side of (16) is negative, and so r_1 must also be negative. According to Remark A.3.2, because $x_1^* > 0$, r_1 need not be nonnegative as is stated in assumption 2 of Theorem A.3.1. Similarly, $x_2^* > 0$ implies that r_2 need not be nonnegative. With r_6 assumed positive, the remaining components of the right eigenvector are positive. Thus, the assumption imposed on the right eigenvector is not violated.

The components of the left eigenvector are given by

$$\begin{aligned} l_1 &= l_2 = 0 \\ l_3 &= \left(\frac{\eta_r\alpha}{N(r+\mu)(\alpha+\mu)} + \frac{\eta_i}{N(\alpha+\mu)}\right) l_6 \\ l_4 &= \frac{\eta_p}{N(r_p+\mu)} l_6 \\ l_5 &= \frac{\eta_r}{N(r+\mu)} l_6, \end{aligned}$$

where l_6 must satisfy $l \cdot r = 1$.

For convenience, we rewrite system (1) using the change of variables $x_1 = S, x_2 = S_p, x_3 = I, x_4 = R_p, x_5 = R, x_6 = z$, letting $x = (x_1, ..., x_6)^T$, and $\frac{dx}{dt} = f(x, \phi)$. Since $l_1 = l_2 = 0$, we in fact only

need $\frac{dx_k}{dt} = f_k(x, \phi)$ for $k \geq 3$ to compute a and b in Theorem A.3.1:

$$\begin{aligned}
f_3 &= \phi^* x_6 x_1 - (\alpha + \mu) x_3 \\
f_4 &= \phi^* (1 - e) x_6 x_2 - (r_p + \mu) x_4 \\
f_5 &= \alpha x_3 - (r + \mu) x_5 \\
f_6 &= \frac{\eta_i x_3 + \eta_p x_4 + \eta_r x_5}{N} (1 - x_6) - g x_6.
\end{aligned}$$

Remembering that $x_k^* = 0$ for $k \geq 3$, we have

$$\begin{aligned}
\frac{\partial f_3}{\partial x_6 \partial x_1} = \phi^* = \frac{\partial f_3}{\partial x_1 \partial x_6} \\
\frac{\partial f_4}{\partial x_6 \partial x_2} = \phi^* (1 - e) = \frac{\partial f_3}{\partial x_2 \partial x_6} \\
\frac{\partial f_6}{\partial x_6 \partial x_3} = -\frac{\eta_i}{N} = \frac{\partial f_6}{\partial x_3 \partial x_6} \\
\frac{\partial f_6}{\partial x_6 \partial x_4} = -\frac{\eta_p}{N} = \frac{\partial f_6}{\partial x_4 \partial x_6} \\
\frac{\partial f_6}{\partial x_6 \partial x_5} = -\frac{\eta_r}{N} = \frac{\partial f_6}{\partial x_5 \partial x_6}
\end{aligned}$$

and

$$\begin{aligned}
\frac{\partial f_3}{\partial x_6 \partial \phi} = x_1^* \\
\frac{\partial f_4}{\partial x_6 \partial \phi} = (1 - e) x_2^*.
\end{aligned}$$

The remaining second partial derivatives are zero. From our calculation of the left and right eigenvectors and second partial derivatives, we obtain

$$\begin{aligned}
a &= 2 l_3 r_6 r_1 \phi^* + 2 s l_4 r_6 r_2 \phi^* (1 - e) - 2 l_6 r_6 \left(\frac{\eta_i r_3 + \eta_p r_4 + \eta_r r_5}{N} \right) \\
b &= l_3 l_6 x_1^* + l_4 r_6 (1 - e) x_2^*
\end{aligned} \tag{17}$$

From the requirement that l_6 satisfy $l \cdot r = 1$, we obtain that l_6 has the same sign as r_6, and consequently $b > 0$. Thus, backward bifurcation occurs if $a > 0$. Rewriting the inequality $a > 0$ in an equivalent form, we find that backward bifurcation occurs only if inequality (4) holds.

□

A.4 Numerical analysis of optimal control system

The complexity of the optimal control problem required that we obtain solutions to the problem numerically. To this end, we implemented the forward-backward sweep method in which one begins the algorithm by making an initial guess at the optimal control pair (u_1^*, u_2^*) and uses this initial guess to solve the state system in forward time. The solution to the state system along with the guessed optimal control pair are then used as inputs to the adjoint system, which must be solved numerically in backwards time using the terminal condition $\lambda(T) = \vec{0}$. The description of the optimal control pair is then updated using the equations in (3) and the state and adjoint systems are integrated using the updated controls. We implemented the fourth-order Runge-Kutta method to perform all numerical integrations with a step size of $dt = .1$ months over a time interval of $T = 120$ months (10 years). At this stage in the algorithm, we calculated the error between the updated control pair and the previous estimate of the control pair along with the error between the new and old solutions to the state and adjoint systems. More precisely, if we denote the updated values of the controls, the solutions to the states system, and the solutions to the adjoint system by u_i, x_i, λ_i, respectively, we calculate the errors

$$\begin{aligned}
\epsilon_1 &= \min_{i\in\{1,2\}} \delta \sum |u_i| - \sum |u_{i_{old}} - u_i| \\
\epsilon_2 &= \min_{i\in\{1,\ldots,6\}} \delta \sum |x_i| - \sum |x_{i_{old}} - x_i| \\
\epsilon_3 &= \min_{i\in\{1,\ldots,6\}} \delta \sum |\lambda_i| - \sum |\lambda_{i_{old}} - \lambda_i|.
\end{aligned}$$

The sums above are taken over the length of the vectors ($T/dt + 1 = 1201$), and in our implementation of the algorithm we set $\delta = .0001$. The calculation of the errors completes one iteration of the algorithm. If $\epsilon := \min\{\epsilon_1, \epsilon_2, \epsilon_3\} < 0$, the algorithm continues to the next iteration, using the updated control pair as the new inputs to the state and adjoint systems and the steps described above are repeated. The algorithm is said to converge when $\epsilon \geq 0$. Note that $\epsilon_1 \geq 0$ is equivalent to $\frac{\sum |u_{i_{old}} - u_i|}{\sum |u_i|} \leq \delta$ as long as $u_i \neq \vec{0}$; thus, we required that the relative errors between old and new values be small, and rewrote the desired inequalities to avoid division by zero.

References

[1] S. T. Agnandji, B. Lell, J. F. Fernandes, B. P. Abossolo, B. G. N. O. Methogo, and A. L. Kabwende. A Phase 3 trial of RTS,S/AS01 malaria vaccine in African infants. *New England Journal of Medicine*, 367(24):2284–2295, 2012. PMID: 23136909.

[2] R. Aguas, L. J. White, R. W. Snow, and M. G. M. Gomes. Prospects for malaria eradication in sub-saharan africa. *PLoS ONE*, 3(3):e1767, 2008.

[3] RM Anderson and RM May. Infectious disease of humans. *Dynamics and control*, 1991.

[4] J. L. Aron. Acquired immunity dependent upon exposure in an SIRS epidemic model. *Mathematical Biosciences*, 88:37–47, 1987.

[5] H. E. Atieli, G. Zhou, Y. Afrane, M. Lee, I. Mwanzo, A. K. Githeko, and G. Yan. Insecticide-treated net (ITN) ownership, usage, and malaria transmission in the highlands of western Kenya. *Parasites & Vectors*, 4(113):1–10, 2011.

[6] Norman TJ Bailey et al. The biomathematics of malaria. the biomathematics of diseases: 1. *The biomathematics of malaria. The Biomathematics of Diseases: 1.*, 1982.

[7] C. Castillo-Chavez and B. Song. Dynamical models of tuberculosis and their applications. *Mathematical Biosciences and Engineering*, 1(2):361–404, 2004.

[8] N. Chitnis, J. M. Cushing, and J. M. Hyman. Bifurcation analysis of a mathematical model for malaria transmission. *SIAM Journal of Applied Mathematics*, 67(1):24–45, 2006.

[9] C. Chiyaka, J. M. Tchuenche, W. Garira, and S. Dube. A mathematical analysis of the effects of control strategies on the transmission dynamics of malaria. *Applied Mathematics and Computation*, 195(2):641–662, 2008.

[10] M. C. de Castro, Y. Yamagata, D. Mtasiwa, M. Tanner, J. Utzinger, J. Keiser, and B. H. Singer. Integrated urban malaria control: a case study in Dar es Salaam, Tanzania. *American Journal of Tropical Medicine and Hygiene*, 71:103 – 117, 2004.

[11] O. Diekmann and J. A. P. Heesterbeek. *Mathematical epidemiology*, chapter Further notes on the basic reproduction number. Springer, 2008.

[12] O. Diekmann, J. A. P. Heesterbeek, and M. G. Roberts. The construction of next-generation matrices for compartmental epidemic models. *J. R. Soc. Intergace*, 2009.

[13] D.L. Doolan, C. Dobano, and J.K. Baird. Acquired immunity to malaria. *Clinical Microbiology Reviews*, 22(1):725–732, 2009.

[14] J. Dushoff, W. Huang, and C. Castillo-Chavez. Backwards bifurcations and catastrophe in simple models of fatal diseases. *Journal of Mathematical Biology*, 36:227–248, 1995.

[15] J. T. Griffin, T. D. Hollingsworth, L. C. Okell, T. S. Churcher, M. White, W. Hinsley, T. Bousema, C. J. Drakeley, N. M. Ferguson, M-G. Basanez, and A. C. Ghani. Reducing plasmodium falciparum malaria transmission in africa: A model-based evaluation of intervention strategies. *PLoS Medicine*, 7(8):e1000324, 2010.

[16] S. Gupta, R. W. Snow, C. A. Donnelly, K. Marsh, and C. Newbold. Immunity to non-cerebral severe malaria is acquired after one or two infections. *Nature Medicine*, 5:340–343, 1999.

[17] M. E. Halloran and C. J. Struchiner. Modeling transmission dynamics of stage-specific malaria vaccines. *Parasitology Today*, 8(3):77–85, 1992.

[18] M. E. Halloran, C. J. Struchiner, and A. Spielman. Modeling malaria vaccines II: Population effects of stage-specific malaria vaccines dependent on natural boosting. *Mathematical Biosciences*, 94:115–149, 1989.

[19] E. Jung, S. Lenhart, and Z. Feng. Optimal control of treatments in a two-strain tuberculosis model. *Discrete and Continuous Dynamical Systems–Series B*, 2(4):475–482, 2002.

[20] G. F. Killeen, F. E. McKenzie, B. D. Foy, C. Schieffelin, P. F. Billingsley, and J. C. Beier. The potential impact of integrated malaria transmission control on entomologic inoculation rate in highly endemic areas. *American Journal of Tropical Medicine and Hygiene*, 62(5):545 – 551, 2000.

[21] J. Langhorne, F. M. Ndungu, A.M. Sponas, and K. Marsh. Immunity to malaria: more questions than answers. *Nature Immunology*, 9(7):13–36, 2008.

[22] S. M. Lenhart and J. T. Workman. *Optimal control applied to biological models*. CRC Press, 2007.

[23] N. Maire, J. J. Aponte, A. Ross, R. Thompson, P. Alonso, J. Utzinger, M. Tanner, and T. Smith. Modeling a field trial of the RTS,SAS02A malaria vaccine. *American Journal of Tropical Medicine and Hygiene*, 75:104–110, 2006.

[24] L. Molineaux and G. Gramiccia. *The Garki project: Research on the epidemiology and control of malaria in the Sudan savanna of West Africa*. World Health Organization, 1980.

[25] K. Raghavendra, T. K. Barik, B. P. N. Reddy, P. Sharma, and A. P. Dash. Malaria vector control: from past to future. *Parasitology Research*, 108:757 – 779, 2011.

[26] T.C. Reluga, J. Medlock, and A.S. Perelson. Backwards bifurcations and multiple equilibria in epidemic models with structured immunity. *Journal of Theoretical Biology*, 252(1):155–165, 2008.

[27] A. Seierstad and K. Sydsaeter. *Optimal control theory with economic applications*. Amsterdam, The Netherlands: North Holland, 1987.